JOURNAL OF STRESS ANALYSIS

Journal of Stress Analysis
Vol. 5, No. 2, Autumn − Winter 2020-21, 101-108

Bu-Ali Sina University

ORIGINAL RESEARCH PAPER

# Numerical Investigation of Energy Absorption of Thin-walled Combined Geometry under Axial and Oblique Loading

**M. Karimi, S.H. Nourbakhsh***

Mechanical Engineering Department, University of Shahrekord, Shahrekord, Iran.

## Article info

*Article history:*
Received 18 January 2021
Received in revised form
13 March 2021
Accepted 17 March 2021

*Keywords:*
Energy absorption
Thin-walled
Combined geometry
Axial and oblique loading
Aluminum

**Abstract**

In this paper, energy absorption of aluminum thin-walled combined geometry, including a cylinder and a hemisphere under axial and oblique loading, is investigated using numerical simulation. The aim of this research is optimizing the dimensions of the combined geometry in order to increase the energy absorption capacity and comparing it with an equal weight thin-walled simple cylinder. Numerical simulations were performed at 0, 7, 14, and 21 degree of loading using ABAQUS software. The results showed that with increasing the radius of curvature and decreasing the height of the combined geometry, energy absorption parameters increase, and in general the combined geometry has better performance than the simple cylinder especially in oblique loading. The SAE and CFE of the optimum combined geometry with dimensions of $R = 25$mm, $h = 25$mm, $H = 181.92$mm, and $D = 50$mm in the 0 and 7 degree of loading is similar and in the 14 and 21 degree of loading increased 300% and 200% respectively in comparison with an equal weight thin-walled simple cylinder.

## 1. Introduction

Nowadays, energy absorption systems are widely used in various industries such as aircraft, ships, elevators, and machinery. The purpose of these systems is to absorb energy from collision force during accidents or impact forces in order to reduce damage to people and equipment. Therefore, selecting a model of these systems that has higher energy absorption is one of the most important issues in this field. A sample of thin-walled energy absorbers are combined geometrical shells that are created from the combination of spherical, conical, and cylindrical shells and are widely used in engineering structures such as the nose cone of planes and projectiles, fuel tanks and pressure vessels. Determination of crushing performance and energy absorption characteristics of these structures under different loading conditions and their deformation rate is very important to ensure the level of protection required by energy absorption.

One of the preliminary studies on cylindrical thin-walled structures was conducted by Alexander [1]. Alexander investigated the approximate solution of the collapse of thin-walled cylindrical shells under axial loading. Tasdemirci [2] investigated the effect of tube ends constraint on the axial crushing behavior of an aluminum tube. Tang et al. [3] investigated the crushing analysis of thin-walled beams with different geometrical sections under lateral impact load. Choubini et al. [4] investigated the energy absorption of thin-walled tubes with circular and square sections under transverse impact load. Their results showed that at

*Corresponding author: S.H. Nourbakhsh (Assistant Professor)
E-mail address: nourbakhsh.sh@eng.sku.ac.ir
http://dx.doi.org/10.22084/jrstan.2021.23929.1176
ISSN: 2588-2597

high energies, square tube has 50% higher specific energy absorption than the circular one and filled tube has 20% higher specific energy absorption than the hollow one. The study of thin-walled lightweight structures with window-shaped patterns was carried out under axial crushing by Song et al. [5]. Alavi Nia and Parsapour [6] studied the energy absorption characteristics of multi-cell thin-walled tubes with square section and showed that the energy absorption capacity of the proposed model was about 227% higher than that of the simple model. Davari et al. [7] investigated the energy absorption of open-cell aluminum foam by simulation and analytical equations. Alavi Nia and Parsapour [8] compared the energy absorption capacity of simple and multi-cell thin-walled tubes. Their results showed that the energy absorption capacity of multicellular sections is higher than that of simple sections. Energy absorption and mean crushing load of grooved thin-walled tubes under axial compression were investigated by Hosseinipour and Daneshi [9]. Montazeri et al. [10] analyzed energy absorption, specific absorbed energy(SAE), and crushing performance of grooved and perforated thin-walled tubes made of different materials under axial loading. Their results showed that perforated tubes made of aluminum have maximum crushing and energy absorption performance. Their results showed that the cap absorbs more energy during less crushing. Ghamarian and Abadi [11] compared the crushing performance of the capped thin-walled tubes with the capless ones and showed that the maximum initial peak force can be controlled. The crushing performance and dynamic and quasi-static deformation behavior of metal spherical shells were studied by Gupta and Venkatesh [12]. Numerical and experimental analysis of thin-walled tube crushing behavior with combined square and circular sections was performed by Shojaeefard et al. [13]. The results showed that changes in section dimensions and model length lead to higher energy absorption of combined shells compared to square and circular ones. Tasdemirci et al. [14] studied numerical and experimental characteristics of energy absorption of combined geometric shells at quasi-static and dynamic strain rates and showed that for models with the same radius, the more the thickness of the model, the more the values of SAE and Pm increase. On the other hand, for models with the same thickness, the more the radius of the model increases, the aforementioned values decrease and increase, respectively. Gupta and Sahu [15] studied the collapse mechanics of combined geometric shells. Their results showed that changing geometry affects the plastic deformation process and consequently changes the displacement force and conditions associated with collapse. Han and Park [16] investigated the collapse behavior of square thin-walled columns subjected to oblique loads. Their results showed that there is a critical angle in which the axial collapse is transformed into a bending collapse. The collapse of windowed and multi-cell square tubes of the same weight under axial and oblique loading was compared by Song and Guo [17]. The results showed that at small angles, loading of windowed square and multi-cell tubes may have worse performance than conventional tubes. Effect of thickness and middle-layer material of laminated fiber metal were investigated by Ansari et al. [18], they concluded that the specimen with three layers of the same thickness yields the best absorption energy performance.

In previous studies, the use of optimization of combined geometries considering the issue of non-increasing weight in these geometries in axial and oblique loading has not been investigated. Therefore, in this research, optimization of a type of combined geometry will be discussed that their important feature is having the same weight as a simple cylinder. For this purpose, in simulations, the geometric dimensions of the structures were changed and energy absorption parameters including absorbed energy, crush force efficiency and deformation were investigated at four different collision angles of 0, 7, 14, and 21 degrees. These angles were selected according to other researchers' reviews [19]. Finally, the obtained parameters were compared for combined geometry with simple cylindrical model and the optimal model was introduced. Furthermore, due to the fact that the thickness of the experimental samples may be changed by processes such as drawing, for the optimum combined geometry, the thickness distribution was considered and energy absorption parameters were examined.

## 2. Numerical Simulation

Aluminum sheet with a thickness of 1.5mm was used for the specimens. The aluminum stress-strain diagram is shown in Fig. 1.

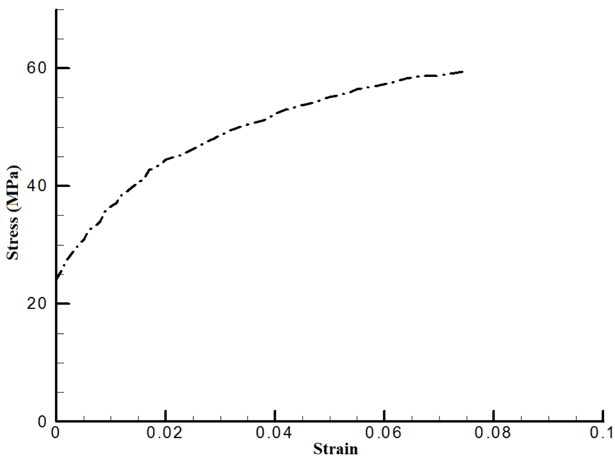


**Fig. 1.** Stress-strain curve of material [8].

The height, outer diameter, and thickness of the thin-walled simple cylinder are 200, 51.5, and 1.5mm, respectively. The combined geometries are composed of two parts: cylindrical and spherical section. Fig. 2 shows the geometric parameters associated with these geometries. Moreover, the values of these parameters are listed in Table 1 for different modes. It is essential to mention that the weight of different combined geometry is equal to simple cylinder.

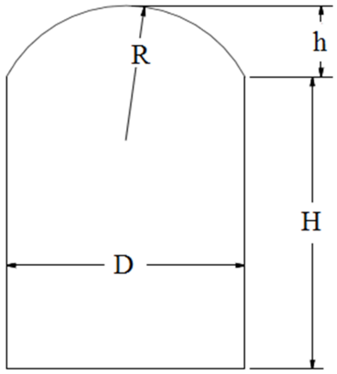


**Fig. 2.** Presentation of geometric parameters of combined geometry.

**Table 1**
The geometric parameters of different mode of combined geometry.

| Code | $R$ (mm) | $h$ (mm) | $H$ (mm) | $D$ (mm) |
|---|---|---|---|---|
| C.S.1 | 20 | 15 | 253.58 | 38.72 |
| C.S.2 | 20 | 20 | 240.48 | 40 |
| C.S.3 | 20 | 25 | 243.51 | 38.72 |
| C.S.4 | 25 | 15 | 210 | 45.82 |
| C.S.5 | 25 | 20 | 190.9 | 48.49 |
| C.S.6 | 25 | 25 | 181.92 | 50 |
| C.S.7 | 30 | 15 | 181.42 | 51.96 |
| C.S.8 | 30 | 20 | 161.13 | 56.56 |
| C.S.9 | 30 | 25 | 148.81 | 59.16 |

The combined geometries are designed in different dimensions according to Table 1 and are named with C.S.1 to C.S.9 codes. Each code represents a sample with specific dimensions. For example, the C.S.4 code represents the shell with dimensions of $R = 25$mm, $h = 15$mm, $H = 210$mm, and $D = 45.82$mm. After ensuring the accuracy of the simulation process by verifying the work of other researchers, the crushing process of the specimens was carried out in different conditions by ABAQUS finite element software in quasi-static state. The simulations were done in axial and oblique loading (7, 14, and 21 degree), these angles were selected according to the ref [19]. The designed model has three parts: upper plate, specimen, and bottom plate in which the top and bottom plates are designed rigidly. The bottom plate is completely fixed while the upper one has movement. Solid element is used for plates and shell element for specimen. The number of optimum elements for deformable specimen was determined about 22,000 S4R elements, the convergence rate is shown in Table 2. To contact the specimen and the top and bottom plates, the surface-to-surface constraint with friction coefficient of 0.2 was used. The finite element model–including the deformable specimen, upper, and bottom plate– is shown in Fig. 3.

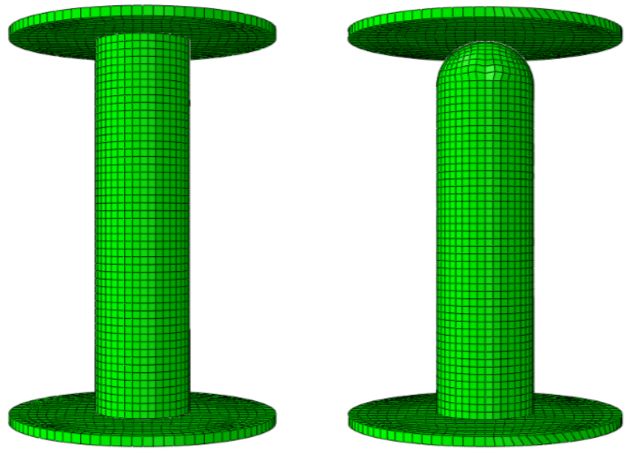


**Fig. 3.** FEM model of, a) Simple cylinder, b) Combined geometry.

## 3. Results and Discussion

In the crushing process, there are important parameters that should be considered in the analysis of the absorbers' performance. One of the most important parameters is the Specific Absorbed Energy (SAE):

$$\mathrm{SAE} = \frac{E}{W} \tag{1}$$

In Eq. (1), $E$ and $W$ are respectively absorbed energy and weight. Absorbed energy is defined as Eq. (2):

$$E = \int_0^\delta P d\delta \tag{2}$$

$P$ and $\delta$ in Eq. (2) are force and displacement, respectively. Moreover, Crush Force Efficiency (CFE) is another important parameter that should be considered in crushing performance:

$$\mathrm{CFE} = \frac{P_m}{P_{\max}} \tag{3}$$

That $P_m$ in Eq. (3) is equal to:

$$P_m = \frac{\int_0^\delta P d\delta}{\delta} \tag{4}$$

**Table 2**
Effect of number of deformable sample elements on the maximum load.

| Number of element | 10000 | 15000 | 22000 | 32000 |
|---|---|---|---|---|
| Maximum load (kN) | 3.2 | 4.8 | 5.2 | 5.35 |

Table 3 shows the values of maximum force, absorbed energy, mean force, SAE, and CFE for simple cylindrical model and combined geometry at angles of 0, 7, 14, and 21 degrees. As can be seen from the results of simple cylinder, by increasing the angle of collision, the efficiency of this type of absorber is practically weakened and it begins to bend instead of absorbing energy. In oblique collisions, there is a critical angle where the absorber begins to bend. By examining the combined geometries, it can be seen that the efficiency is higher than the simple cylinder at different collision angles and the critical angle for the onset of bending increases.

Crush Force Efficiency (CFE) is an important parameter in the evaluation of absorbers. The larger mean force indicates greater energy absorption while trying to reduce the initial maximum force, so the large amount of CFE is very important. As can be seen from the numbers in Table 3, the CFE value of the combined geometries has not decreased compared to simple cylinder, but has also increased significantly in oblique collisions.

**Table 3**
Numerical values obtained from simulation for all specimens at different angles.

| | Crush angle | $P_{\max}$ (kN) | $P_m$ (kN) | CFE (%) | SAE (kJ/kg) |
|---|---|---|---|---|---|
| Cylinder | 0 | 10.41 | 6.40 | 61.51 | 10.03 |
| | 7 | 8.96 | 5.89 | 65.73 | 9.58 |
| | 14 | 6.61 | 2.20 | 33.32 | 3.48 |
| | 21 | 4.85 | 1.81 | 37.22 | 2.48 |
| C.S.1 | 0 | 11.11 | 5.64 | 50.76 | 11.90 |
| | 7 | 8.06 | 5.73 | 71.12 | 11.66 |
| | 14 | 7.13 | 5.56 | 77.97 | 11.37 |
| | 21 | 2.24 | 0.74 | 32.80 | 1.02 |
| C.S.2 | 0 | 9.64 | 5.79 | 60.08 | 11.46 |
| | 7 | 7.39 | 5.45 | 73.84 | 10.83 |
| | 14 | 8.23 | 5.47 | 66.48 | 11.07 |
| | 21 | 2.51 | 0.70 | 28.02 | 1.32 |
| C.S.3 | 0 | 9.80 | 5.51 | 56.22 | 11.57 |
| | 7 | 7.45 | 5.62 | 75.47 | 11.83 |
| | 14 | 4.81 | 0.97 | 20.16 | 2.10 |
| | 21 | 8.67 | 5.43 | 62.60 | 10.71 |
| C.S.4 | 0 | 11.49 | 5.63 | 48.96 | 9.72 |
| | 7 | 9.86 | 5.82 | 59.04 | 9.60 |
| | 14 | 6.19 | 1.90 | 30.63 | 3.53 |
| | 21 | 9.31 | 5.49 | 58.98 | 8.66 |
| C.S.5 | 0 | 9.89 | 5.78 | 58.43 | 9.46 |
| | 7 | 8.04 | 5.95 | 73.92 | 9.43 |
| | 14 | 8.57 | 6.06 | 70.65 | 9.62 |
| | 21 | 7.94 | 5.05 | 63.62 | 5.95 |
| C.S.6 | 0 | 10.02 | 6.11 | 60.97 | 9.59 |
| | 7 | 9.64 | 6.06 | 62.79 | 9.60 |
| | 14 | 8.76 | 6.07 | 69.33 | 9.70 |
| | 21 | 8.19 | 5.95 | 72.68 | 8.53 |
| C.S.7 | 0 | 11.98 | 5.97 | 49.86 | 9.08 |
| | 7 | 8.41 | 5.83 | 69.34 | 8.55 |
| | 14 | 7.58 | 3.04 | 40.10 | 4.86 |
| | 21 | 5.20 | 2.00 | 38.46 | 2.71 |
| C.S.8 | 0 | 9.98 | 5.76 | 57.71 | 7.65 |
| | 7 | 8.43 | 6.01 | 71.25 | 7.89 |
| | 14 | 8.63 | 6.20 | 71.84 | 8.56 |
| | 21 | 8.01 | 5.93 | 74.02 | 7.16 |
| C.S.9 | 0 | 9.74 | 6.07 | 62.29 | 8.25 |
| | 7 | 9.79 | 6.18 | 63.18 | 8.26 |
| | 14 | 8.46 | 6.10 | 72.08 | 7.88 |
| | 21 | 7.86 | 4.24 | 53.91 | 4.77 |

Another case seen from the results of Table 3 is the increase in SAE level of specimens associated with the combined geometry compared to the simple cylinder, which also proves the efficiency of these types of geometries. In order to identify and select the best dimensions for the combined geometry, it should be noted that all the parameters involved in the geometric dimensions are interdependent, which is due to keeping the weight constant relative to the simple cylinder. In general, according to the results, it can be concluded that the more the curvature radius increases and the height decreases, the energy absorption parameters will be improved. After reviewing the results in Table 3, considering the SAE and CFE values simultaneously, it can be seen that C.S.6 shows better efficiency than other specimens at all collision angles. In Fig. 4, the force-displacement diagram is shown for the simple cylinder and C.S.6. As can be seen in this figure, C.S.6 has a smaller initial maximum force and a larger mean force than the simple cylinder, and has not bent at any of the collision angles and has continued to absorb energy. In Table 4, the crushed form of the simple cylinder and C.S.6 can be seen.

**Table 4**
Comparison between crush form of simple cylinder and C.S.6.

| C.S.6 | Simple cylinder | Oblique |
|---|---|---|
| 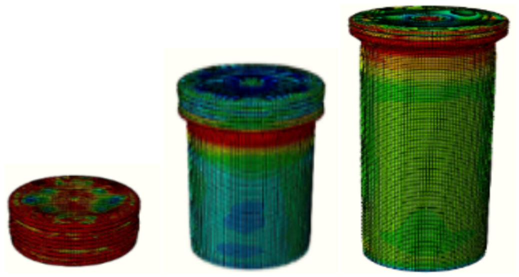 | 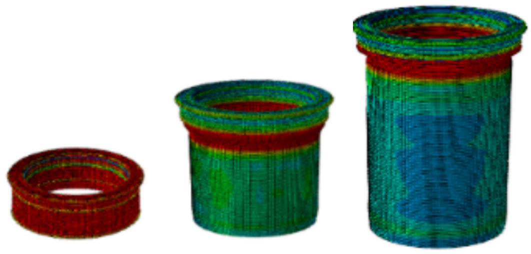 | 0 |
| 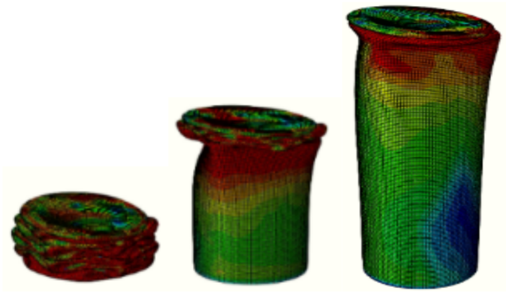 | 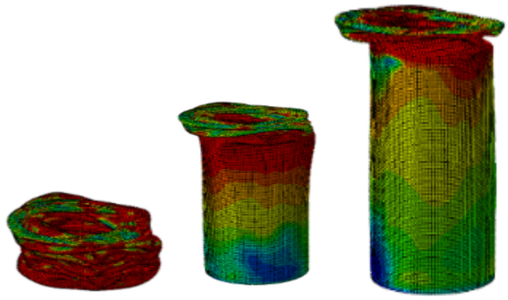 | 7 |
| 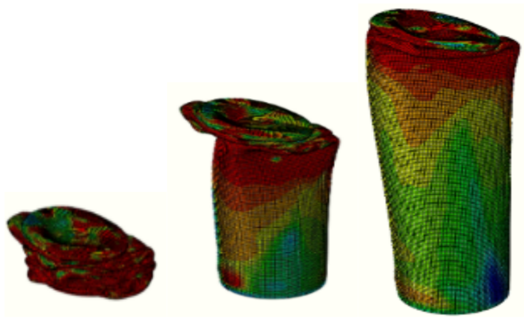 | 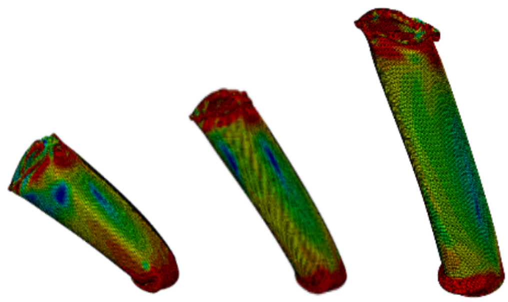 | 14 |
| 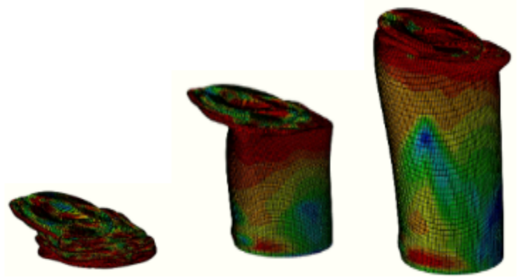 | 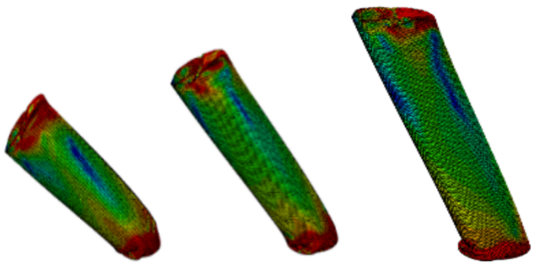 | 21 |

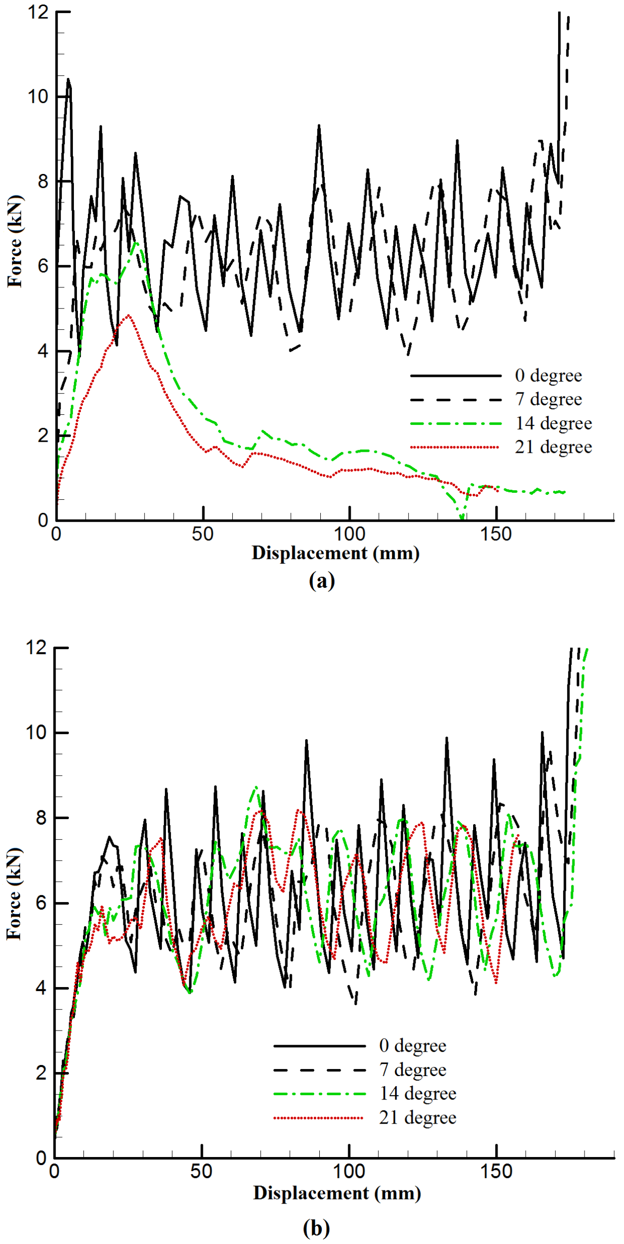


**Fig. 4.** The force-displacement diagram, a) Simple cylinder, b) C.S.6.

In order to compare the results of energy absorption of samples quantitatively, Figs. 5 and 6 show the histograms related to SAE and CFE values for simple cylindrical shell and C.S.6, respectively. According to Fig. 5, it can be seen that SAE value for simple cylindrical shell and C.S.6 at angles of 0 and 7 degrees is almost the same. While at angle of 14, the SAE value of C.S.6 increased about 280% compared to simple cylindrical shell. This amounts to about 345% at 21 degree angle. In addition, C.S.6 has shown better energy absorption at angle of 14 than other angles. On the other hand, at 21 degree, the SAE value for the C.S.6 has decreased by about 13% due to approaching the critical angle compared to the other three.

Fig. 6 shows that the C.S.6 has significant CFE values at 14 and 21 degree compared to the simple cylindrical shell. In these angles, the CFE value increased by about 208% and 195%, respectively. In addition, by increasing the angle from 0 to 21 degrees, CFE values for C.S.6 increased. However, the simple cylinder was significantly reduced by CFE due to lack of energy absorption at two angles of 14 and 21 degreee.

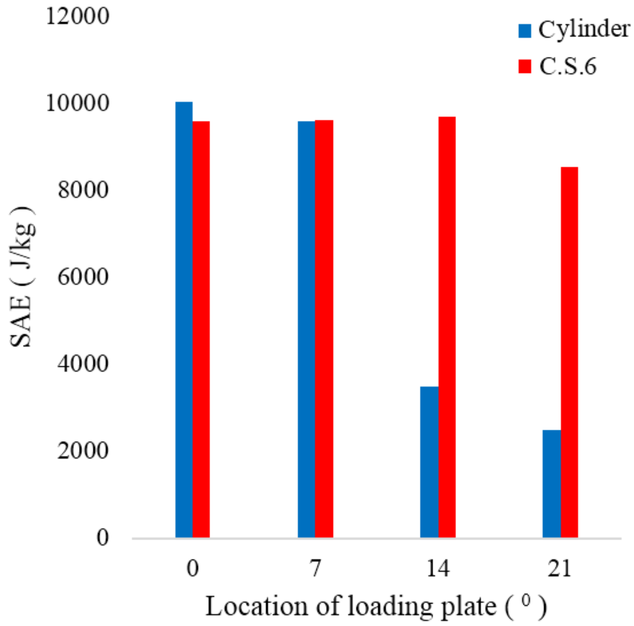


**Fig. 5.** Specific absorbed energy in different angles of loading.

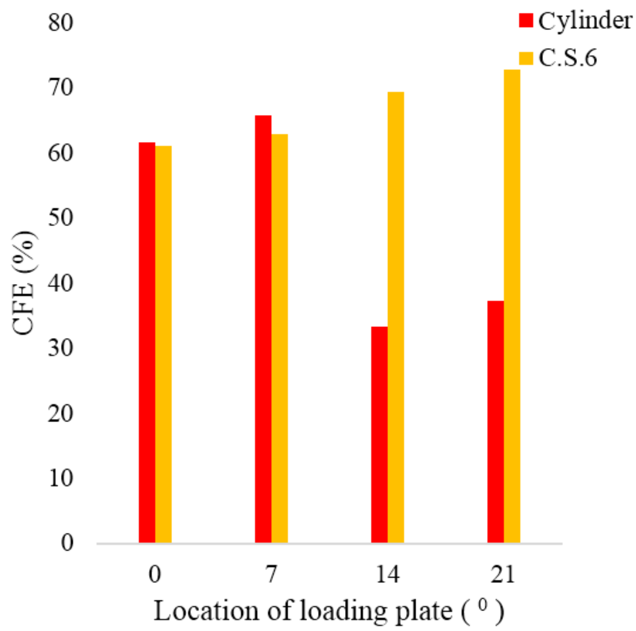


**Fig. 6.** Crush force efficiency in different angles of loading.

One of the factors that may occur in the construction of experimental samples is the issue of thickness changes. Due to the fact that these samples can be produced by the deep drawing process, the sheet thickness changes from the beginning to the end of the sample.

Therefore, the thickness of optimum combined geometry sample (C.S.6) was considered variable and the results related to energy absorption were examined. Fig. 7 shows the changes in the thickness of the sample, which is considered linearly from 0.75 to 1.5mm.

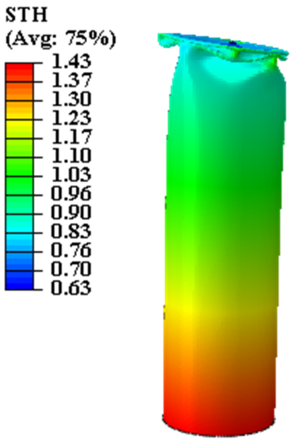


**Fig. 7.** Thickness changes of optimum combined geometry.

Fig. 8 shows the force-displacement diagrams for the optimum combined geometry with variable thickness. As can be seen in this figure, the energy absorption starts from the lower force (approximately ten percent lower), in comparison with Fig. 4b, where the thickness is uniform. In terms of initial force and reduction in transmitted acceleration, the efficiency of this type of samples is acceptable but in viewpoint of specific energy absorption the efficiency of this type of samples is decreasing. The SAE values for the variable thickness samples decrease to 7.1, 6.8, 6.2, and 5.1kJ/kg for 0,7,14, and 21 degree of loading, respectively.

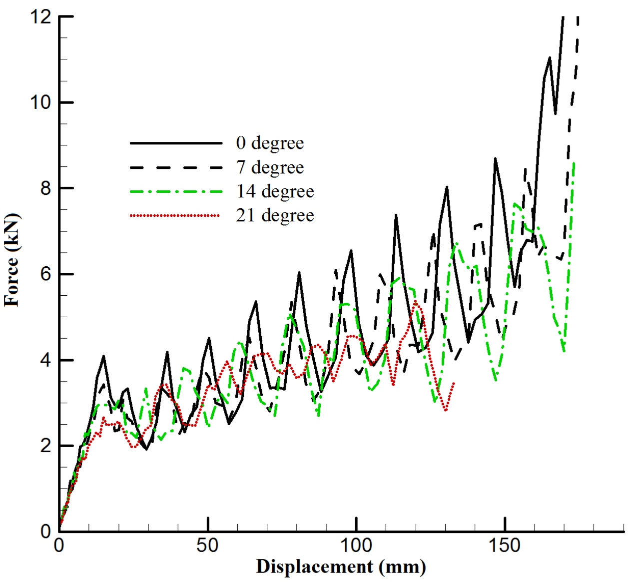


**Fig. 8.** The axial force-displacement diagram for the optimum combined geometry with variable thickness.

## 4. Conclusions

In this study, energy absorption and deformation parameters of thin-walled aluminum tubes with combined geometrical structure and two cylindrical and aspheric sections under axial and oblique loading and the comparison with a simple cylindrical of the same color were investigated. Simulation of energy absorption process for samples was performed at angles of 0, 7, 14, and 21 by ABAQUS finite element software. The most important results of this study are as follows:

- By creating combined geometries consisting of a cylinder and a spherical section, the energy absorption parameters increase.
- Combined geometries have the same efficiency as the simple cylinder of same weight in axial collisions, but they have much higher efficiency in oblique collisions.
- By optimizing the dimensions of combined geometries, the amount of energy absorption can increase by keeping the weight constant.
- The C.S.6 combined shell has a higher energy absorption, SAE and CFE in comparison with other samples
- In average status, the SAE value of C.S.6 is about 147% and its CFE value is about 135% higher than those of simple cylinder.
- By considering the variable thickness for the samples, the efficiency of the adsorbents can greatly increase in terms of reducing the initial force and the transmitted acceleration. But this variable thickness causes a decrease in the amount of specific absorbed energy.

## Acknowledgment

The authors would like to appreciate the use of high performance computing (HPC) center of Shahrekord University.

## References

[1] J.M. Alexander, An approximate analysis of the collapse of thin cylindrical shells under axial loading, Q. J. Mech. Appl. Math., 13(1) (1960) 10-15.

[2] A. Tasdemirci, The effect of tube end constraining on the axial crushing behavior of an aluminum tube, Mater. Des., 29(10) (2008) 1992-2001.

[3] T. Tang, W. Zhang, H. Wang, Crushing analysis of thin-walled beams with various section geometries under lateral impact, Thin-Walled Struct., 102 (2016) 43-57.

[4] M. Choubini, G.H. Liaghat, M. Pol, Investigation of energy absorption and deformation of thin walled tubes with circle and square section geometries under transverse impact loading, Modares Mechanical Engineering, 15(1) (2015) 75-83.

[5] J. Song, Y. Chen, G. Lu, Light-weight thin-walled structures with patterned windows under axial crushing, Int. J. Mech. Sci., 66 (2013) 239-248.

[6] A. Alavi Nia, M. Parsapour, An investigation on the energy absorption characteristics of multi-cell square tubes, Thin-Walled Struct., 68 (2013) 26-34.

[7] S. Davari, S.A. Galehdari, A. Atrian, Design and analysis of graded open-cell aluminum foam shock absorber for helicopter seats during emergency landing conditions, J. Stress Anal., 4(2) (2020) 81-91.

[8] A. Alavi Nia, M. Parsapour, Comparative analysis of energy absorption capacity of simple and multi-cell thin-walled tubes with triangular, square, hexagonal and octagonal sections, Thin-Walled Struct., 74 (2014) 155-165.

[9] S.J. Hosseinipour, G.H. Daneshi, Energy absorbtion and mean crushing load of thin-walled grooved tubes under axial compression, Thin-Walled Struct., 41(1) (2003) 31-46.

[10] S. Montazeri, M. Elyasi, A. Moradpour, Investigating the energy absorption, SEA and crushing performance of holed and grooved thin-walled tubes under axial loading with different materials, Thin-Walled Struct., 131 (2018) 646-653.

[11] A. Ghamarian, M.T. Abadi, Axial crushing analysis of end-capped circular tubes. Thin-Walled Struct., 49(6) (2011) 743-752.

[12] N.K. Gupta, Venkatesh, Experimental and numerical studies of dynamic axial compression of thin walled spherical shells, Int. J. Impact Eng., 30(8-9) (2004) 1225-1240.

[13] M.H. Shojaeefard, A. Najibi, M. Anbarloei, M. Yeganeh, Experimental and numerical crashworthiness investigation of combined circular and square sections, J. Mech. Sci. Technol., 28(3) (2014) 999-1006.

[14] A. Tasdemirci, S. Sahin, A. Kara, K. Turan, Crushing and energy absorption characteristics of combined geometry shells at quasi-static and dynamic strain rates: Experimental and numerical study, Thin-Walled Struct., 86 (2015) 83-93.

[15] P.K. Gupta, R.R. Sahu, A study on mechanics of collapse of combined geometry metallic shells, Thin-Walled Struct., 126 (2018) 48-57.

[16] D.C. Han, S.H. Park, Collapse behavior of square thin-walled columns subjected to oblique loads, Thin-Walled Struct., 35(3) (1999) 167-184.

[17] J. Song, F. Guo, A comparative study on the windowed and multi-cell square tubes under axial and oblique loading, Thin-Walled Struct., 66 (2013) 9-14.

[18] E. Ansari, G.H. Majzoobi, K. Rahmani, M. Kashfi, The effect of middle layer material and thickness on the quasi-static energy absorption of FML, J. Sci. Technol. Compos., 5(3) (2018) 427-436.

[19] A. Alavi Nia, K.H. Fallahnezhad, H. Badnava, H.R. Farhoudi, Effects of buckling initiators on mechanical behavior of thin-walled square tubes subjected to oblique loading, Thin-Walled Struct., 59 (2012) 87-96.